

Dalton Transactions

Accepted Manuscript



This is an *Accepted Manuscript*, which has been through the Royal Society of Chemistry peer review process and has been accepted for publication.

Accepted Manuscripts are published online shortly after acceptance, before technical editing, formatting and proof reading. Using this free service, authors can make their results available to the community, in citable form, before we publish the edited article. We will replace this *Accepted Manuscript* with the edited and formatted *Advance Article* as soon as it is available.

You can find more information about *Accepted Manuscripts* in the [Information for Authors](#).

Please note that technical editing may introduce minor changes to the text and/or graphics, which may alter content. The journal's standard [Terms & Conditions](#) and the [Ethical guidelines](#) still apply. In no event shall the Royal Society of Chemistry be held responsible for any errors or omissions in this *Accepted Manuscript* or any consequences arising from the use of any information it contains.

Assessing Ligand Selectivity for Uranium over Vanadium Ions to Aid in the Discovery of Superior Adsorbents for Extraction of UO_2^{2+} from Seawater

Alexander S. Ivanov and Vyacheslav S. Bryantsev*

Oak Ridge National Laboratory, Chemical Sciences Division, 1 Bethel Valley Rd., Oak Ridge, Tennessee, 37831-6119, United States

Corresponding Author:

*Email: bryantsevv@ornl.gov

Phone: (865) 5761753

Notes:

The United States Government retains and the publisher, by accepting the article for publication, acknowledges that the United States Government retains a nonexclusive, paid-up, irrevocable, worldwide license to publish or reproduce the published form of this manuscript, or allow others to do so, for United States Government purposes. The Department of Energy will provide public access to these results of federally sponsored research in accordance with the DOE Public Access Plan (<http://energy.gov/downloads/doe-public-access-plan>).

ABSTRACT

Uranium is used as the basic fuel for nuclear power plants, which generate significant amounts of electricity and have life cycle carbon emissions that are as low as renewable energy sources. However, the extraction of this valuable energy commodity from the ground remains controversial, mainly because of environmental and health impacts. Alternatively, seawater offers an enormous uranium resource that may be tapped at minimal environmental cost. Nowadays, amidoxime polymers are the most widely utilized sorbent materials for large-scale extraction of uranium from seawater, but they are not perfectly selective for uranyl, UO_2^{2+} . In particular, the competition between UO_2^{2+} and $\text{VO}^{2+}/\text{VO}_2^+$ cations poses a significant challenge to the efficient mining of UO_2^{2+} . Thus, screening and rational design of more selective ligands must be accomplished. One of the key components in achieving this goal is the establishment of computational techniques capable of assessing ligand selectivity trends. Here, we report an approach based on quantum chemical calculations that achieves high accuracy in reproducing experimental aqueous stability constants for $\text{VO}^{2+}/\text{VO}_2^+$ complexes with ten different oxygen donor ligands. The predictive power of the developed computational protocol is demonstrated for amidoxime-type ligands, providing greater insights into new design strategies for the development of the next generation of adsorbents with high selectivity toward UO_2^{2+} over $\text{VO}^{2+}/\text{VO}_2^+$ ions. Importantly, the results of calculations suggest that alkylation of amidoxime moieties present in poly(acrylamidoxime) sorbents can be a potential route to better discrimination between the uranyl and competing vanadium ions in seawater.

INTRODUCTION

Uranium is the key element for electricity generation through nuclear power. Traditional methods of uranium recovery are usually based on the process of extracting uranium ore from the ground, including open pit, underground, and in situ leach mining, all of which cause severe environmental pollution.¹ Therefore, increasing production of nuclear power will inevitably lead to an even bigger impact on the environment. Moreover, the world's total uranium supply from mines is not sufficient to sustain more than 100 years of power generation at the current consumption rates.² Fortunately, vast amounts of uranium, roughly 1000 times the known reserves of mined uranium, are dissolved in the world's oceans,³ largely in the form of

$\text{UO}_2(\text{CO}_3)_3^{4-}$ - uranyl tricarbonate,⁴ and, in contrast to terrestrial resources, may be tapped at minimal environmental cost. However, extraction of uranyl is extremely challenging because it is present at very low concentrations ($3.3 \mu\text{g L}^{-1}$) in seawater.⁵ Although many materials and methods have been developed⁶⁻¹⁰ for the recovery of uranyl from seawater, sorption of UO_2^{2+} by polymers functionalized with amidoxime-type ligands has shown the greatest promise.¹¹⁻¹³ According to a recent report,¹⁴ the current generation of adsorbents is capable of capturing as high as 3.3 mg U per g adsorbent after ~60 days of contact with seawater. However, poly(acrylamidoxime) fibers are not perfectly selective for UO_2^{2+} . In particular, the high vanadium uptake¹⁵ (~3 times higher than uranium) found in real seawater experiments suggests that vanadium ions are competing with uranyl for adsorption to the amidoxime-based sorbent. Indeed, sorption studies^{16,17} have demonstrated that vanadium is strongly absorbed by poly(acrylamidoxime) fibers, diminishing the effective sites that are available for uranium and thus significantly reducing the sorption capacity and efficiency. Furthermore, the strongly acidic conditions required to elute vanadium cations from the sorbent lower the reusability of the sorbent and eventually lead to its damage.^{16,17} Therefore, rational design of new chelating agents with enhanced binding affinity and selectivity for uranyl over $\text{VO}^{2+}/\text{VO}_2^+$ ions is expected to help in achieving the overall goal of UO_2^{2+} recovery without sacrificing durability of the sorbent. However, current experimental efforts toward UO_2^{2+} -selective ligand discovery are usually based on the so-called trial-and-error approach and thus require a huge amount of time and resources. Alternatively, computational predictions can provide a more systematic, rapid, inexpensive, and reliable method for the prospective design and screening of superior ligands for selective sequestration of uranium from seawater. While many computational works on uranyl complexation with various ligands have been performed,¹⁸⁻²⁴ to the best of the authors' knowledge, there have been no theoretical studies regarding quantitative evaluation of ligand selectivity for UO_2^{2+} over competing ions. In the following work, we present a straightforward approach, based on quantum chemical calculations, that is able to prioritize ligands with strong binding affinity and high selectivity toward UO_2^{2+} over VO^{2+} and VO_2^+ ions. The approach is also utilized to test new design principles for improving the UO_2^{2+} *versus* $\text{VO}^{2+}/\text{VO}_2^+$ separation ability of amidoxime-type ligands.

METHODS

Electronic structure calculations were performed with the Gaussian 09 D.01 software.²⁵ We adopted the density functional theory (DFT) approach for our calculations using the B3LYP^{26,27} and M06²⁸ density functionals with the standard Stuttgart small-core (SSC) 1997 relativistic effective core potential (RECP),²⁹ the associated contracted [6s/5p/3d/1f] and [8s/7p/6d/4f] basis sets for vanadium and uranium atoms, respectively, and the 6-311++G(d,p) basis set for the light atoms. Frequency calculations were performed at the B3LYP/SSC/6-31+G(d) level to ensure that geometries were minima and to compute zero-point energies and thermal corrections using a methodology introduced by Truhlar et al.,³⁰ which is based on the so-called quasiharmonic approximation – the usual harmonic oscillator approximation, except that vibrational frequencies lower than 30 cm⁻¹ were raised to 30 cm⁻¹ as a way to correct for the well-known breakdown of the harmonic oscillator model for the free energies of low-frequency vibrational modes. Using the gas-phase geometries, implicit solvent corrections were obtained at 298 K with the SMD³¹ solvation model as implemented in Gaussian 09 at the B3LYP/SSC/6-31+G(d) level of theory. Since only the first coordination shell was treated explicitly in this study, it was possible to perform a systematic search of low-energy clusters for a given composition. The results are reported using the lowest energy clusters identified at the B3LYP/SSC/6-31+G(d) level for a given stoichiometry and binding motif. Optimized atomic coordinates and energies for all reported structures, as well as a sample Gaussian 09 input file, are provided as Electronic Supplementary Information.

The preference for using a combination of the B3LYP and the M06 functionals with the SMD solvation model was based on the results of our previous studies,^{32,33} which showed that the chosen level of theory provides the best overall performance in predicting the log K_I values of uranyl complexes with anionic oxygen and amidoxime donor ligands. In addition, single-point coupled-cluster theory calculations, CCSD(T)/aug-cc-pvDZ (the valence electrons on C, O, H and the valence and subvalence electrons (3s, 3p) on V were correlated), using B3LYP/aug-cc-pvDZ optimized geometries were employed for VO²⁺ and VO₂⁺ complexes with acetate and oxalate ligands.

Complexation free energies in aqueous solution, ΔG_{aq} , and stability constants, log K_I , were calculated using the methodology described in our previous work on uranyl containing complexes.³³ According to the thermodynamic cycle shown in **Scheme 1**, ΔG_{aq} is given by:

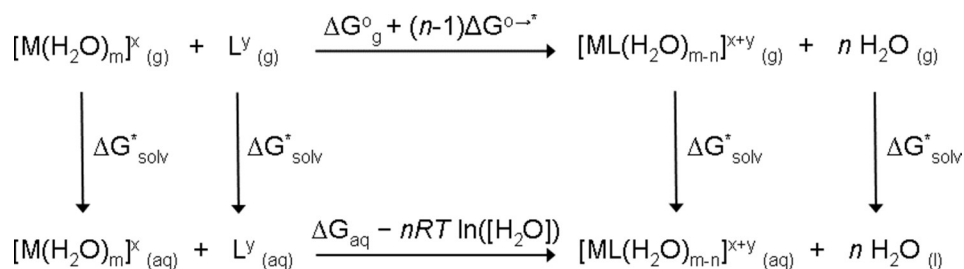
$$\Delta G_{\text{aq}} = \Delta G_{\text{g}}^{\circ} + \Delta \Delta G_{\text{solv}}^* + (n-1)\Delta G^{\circ \rightarrow *} + nRT \ln([\text{H}_2\text{O}])$$

where $\Delta G_{\text{g}}^{\circ}$ is the free energy of complexation in the gas phase and $\Delta \Delta G_{\text{solv}}^*$ is the difference in the solvation free energies for a complexation reaction:

$$\Delta \Delta G_{\text{solv}}^* = \Delta G_{\text{solv}}^*([\text{ML}(\text{H}_2\text{O})_{m-n}]^{x+y}) + n\Delta G_{\text{solv}}^*(\text{H}_2\text{O}) - \Delta G_{\text{solv}}^*([\text{M}(\text{H}_2\text{O})_m]^x) - \Delta G_{\text{solv}}^*(\text{L}^y)$$

where L^y denotes the ligand with a charge of y and M can be VO^{2+} or VO_2^+ . The standard state correction terms must be introduced to connect $\Delta G_{\text{g}}^{\circ}$, $\Delta \Delta G_{\text{solv}}^*$, and ΔG_{aq} , which are defined using different standard state conventions. The free energy change for the conversion of 1 mol of solute from the gas phase at a standard state of 1 atm (24.46 L/mol) to the aqueous phase at a standard state of 1 mol/L at 298.15 K is given by $\Delta G^{\circ \rightarrow *} = 1.89$ kcal/mol. Likewise, $RT \ln([\text{H}_2\text{O}]) = 2.38$ kcal/mol ($T = 298.15$ K) is the free energy change for the conversion of 1 mol of solvent from the aqueous phase at 1 mol/L to pure water at a standard state of 55.34 mol/L. Lastly, the stability constant ($\log K_1$) value is related to free energy change for the complexation

reaction by the following equation: $\log K_1 = \frac{-\Delta G_{\text{aq}}}{2.303 \cdot RT}$



Scheme 1. Thermodynamic cycle used to calculate ΔG_{aq} .

Coefficients (“a” and “b”) in linear regression equations ($y = a + bx$) were calculated by the least-squares method. In addition, p -values were computed to assess the significance of the coefficients. “a” and “b” were considered to be significant if the p -value was less than the significance level ($\alpha = 0.05$). Otherwise, the coefficients were disregarded. Coefficient “a” turned out to be insignificant for regression equation (a) (see Fig. 2) derived for the VO^{2+} complexes and thus it was eliminated from the regression equation.

RESULTS AND DISCUSSION

Structural and thermodynamic studies, including single crystal X-ray diffractometry, UV/Vis spectroscopy, potentiometry, and microcalorimetry can be used to assess the competition between UO_2^{2+} and other seawater cations in the sequestration process.^{34,35} For instance, the stability constants, $\log K$, determined in these studies can help explain and predict the sorption behavior of these cations with amidoxime ligands and thus evaluate the potential of novel, more selective and robust sorbents for uranium extraction.³⁶ In an effort to propose new design strategies aimed at improving the ligand selectivity for UO_2^{2+} over $\text{VO}^{2+}/\text{VO}_2^+$ ions, we have applied density functional theory (DFT) calculations to establish a computational protocol capable of predicting stability constants, $\log K_I$, for 1:1 vanadium ion : ligand complexes.

Two sets, each consisting of 10 negative oxygen donor ligands depicted in Fig. 1, were selected to test the ability of the adopted computational method to reproduce experimental stability constant values for the corresponding VO^{2+} and VO_2^+ complexes. In contrast to the experimental data for uranium complexes available in the Smith and Martell's compilation of Critical Stability Constants series,³⁷ the reports on the experimental $\log K_I$ values for VO^{2+} and VO_2^+ complexes are quite limited, indicating that the accurate measurement of $\text{VO}^{2+}/\text{VO}_2^+$ stability constants is difficult. Results reported in other sources are often deficient in specifying essential reaction conditions (e.g., temperature, ionic strength, nature of supporting electrolyte) and cannot be recommended, for they cannot be reproduced in other laboratories, and unfortunately much of the reported data for vanadium complexes falls into this category. Hence, the choice of the particular sets of ligands (Fig. 1) was based on the availability of experimental aqueous stability constant data that meet the criteria for critical selection.³⁷ In cases where $\log K_I$ values were not available at zero ionic strength, they were corrected to zero ionic strength using the Davies equation.³⁸ The experimental $\log K_I$ values for VO^{2+} and VO_2^+ complexes, spanning a range of nearly 11 orders of magnitude, are tabulated in Tables 1 and 2, respectively.

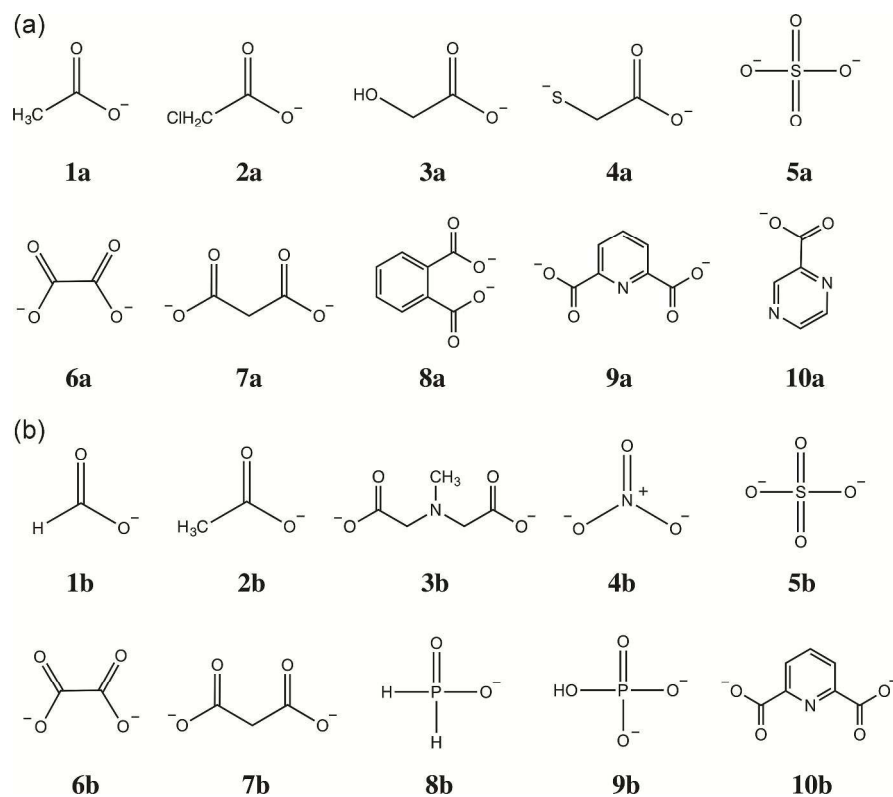


Fig. 1. Sets of negative oxygen donor ligands used to calculate stability constants, $\log K_I$, values for corresponding (a) oxovanadium (IV) and (b) dioxovanadium (V) complexes.

Table 1. Comparison of Experimental, Calculated, and Predicted $\log K_I$ Values for Oxovanadium (IV) Complexes with Oxygen Donor Ligands.

ligand	expt. ^a $\log K_I$	calc. ^b $\log K_I$	abs. error	pred. ^c $\log K_I$	abs. error
1a acetate	2.6	12.6	10.0	3.4	0.8
2a chloroacetate	1.7	7.4	5.7	2.0	0.3
3a glycolate	3.2	10.8	7.6	2.9	0.3
4a thioglycolate	8.8	33.3	24.5	9.1	0.3
5a sulfate	2.4	11.3	8.9	3.1	0.7
6a oxalate	7.0	22.1	15.1	6.0	1.0
7a malonate	6.7	23.7	17.0	6.5	0.2
8a phthalate	4.9	19.8	14.9	5.4	0.5
9a dipicolinate	8.0	28.8	20.8	7.8	0.2
10a pyrazinecarboxylate	3.9	13.3	9.4	3.6	0.3

^aCorrected to zero ionic strength with the Davies equation.³⁸

^bCalculated using ΔG_{aq} .

^cPredicted from correlations shown in Fig. 2.

Table 2. Comparison of Experimental, Calculated, and Predicted $\log K_I$ Values for Dioxovanadium (V) Complexes with Oxygen Donor Ligands.

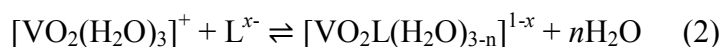
ligand	expt. ^a $\log K_I$	calc. ^b $\log K_I$	abs. error	pred. ^c $\log K_I$	abs. error
1b formate	1.7	7.9	6.2	1.5	0.2
2b acetate	2.6	11.2	8.6	2.8	0.2
3b methyliminodiacetate	10.8	28.3	17.5	9.5	1.3
4b nitrate	-0.2	0.5	0.7	-1.4	1.2
5b sulfate	1.6	9.4	7.8	2.1	0.5
6b oxalate	6.6	18.3	11.7	5.6	1.0
7b malonate	5.2	19.4	14.2	6.0	0.8
8b hypophosphite	1.5	11.1	9.6	2.7	1.2
9b hydrogen phosphate	5.2	19.4	14.2	6.0	0.8
10b dipicolinate	9.3	28.6	19.3	9.6	0.3

^aCorrected to zero ionic strength with the Davies equation.³⁸

^bCalculated using ΔG_{aq} .

^cPredicted from correlations shown in Fig. 2.

Using an approach involving the application of a standard thermodynamic cycle (Scheme 1), the complexation free energies in aqueous solution, ΔG_{aq} , were evaluated according to equilibrium reactions given by eqs 1 and 2:



The ΔG_{aq} calculations require the global minimum geometries for each species. Given that the lowest energy configurations of the solvated VO^{2+} and VO_2^+ ions have been previously identified,^{39,40} and the free anionic ligands, L^{x-} , are simple and rigid enough to be represented by a single conformation, the main issue was to find the most stable forms for $[\text{VOL}(\text{H}_2\text{O})_{4-n}]^{2-x}$ and $[\text{VO}_2\text{L}(\text{H}_2\text{O})_{3-n}]^{1-x}$ complexes. Since only the first coordination shell of the vanadium complexes was treated explicitly, it was possible to perform a systematic search of low-energy clusters for a given composition. The bidentate coordination with the $\text{VO}^{2+}/\text{VO}_2^+$ ions was found to be predominant over the monodentate coordination that was observed only for VO_2^+ complex with hypophosphite ligand. The complexation with ligands containing additional nitrogen donor atom, namely, methyliminodiacetate and dipicolinate (Fig. 1), resulted in a tridentate binding to the vanadium ions. With respect to the number of water molecules bound to the vanadium atom, the

results of calculations demonstrate that the most stable arrangement represents the five-coordinate structures. In other words, bidentate binding displaces two water molecules from the hydrated VO^{2+} and VO_2^+ complexes leading to the formation of $[\text{VOL}(\text{H}_2\text{O})_2]^{2-x}$ and $[\text{VO}_2\text{L}(\text{H}_2\text{O})]^{1-x}$ species, respectively; whereas monodentate binding can replace only one water. The observed coordination number is in accord with crystal structure data showing that a coordination number five is typical for the vanadium complexes with rigid and sterically strained ligands.^{39,40}

The calculated stability constant, $\log K_I^{\text{calc}}$, values for the VO^{2+} and VO_2^+ complexes are summarized in Tables 1 and 2, respectively. As expected, our DFT-based method permitted reasonably good estimates of relative binding strengths of VO^{2+} and VO_2^+ complexes, while the absolute complexation energies were significantly overestimated, leading to inaccurately high $\log K_I$ values (calc. $\log K_I$ values in Tables 1 and 2). Consistent with DFT, high-level CCSD(T)/aug-cc-pvDZ//B3LYP/aug-cc-pvDZ calculations for acetate- $\text{VO}^{2+}/\text{VO}_2^+$ and oxalate- $\text{VO}^{2+}/\text{VO}_2^+$ complexes also overpredicted the $\log K_I$ values (Table S1 of the ESI†), suggesting that the employed computational methodology (density functionals and basis sets) is not the main source of errors in the ΔG_{aq} calculations. The overestimated $\log K_I$ is the consequence of the simplification in solvent description used in our cluster models, since the solvation free energy of a multivalent ion is not fully accounted for by treating only the first hydration shell around the metal ion explicitly.⁴¹ However, accurate predictions of the absolute $\log K_I$ values (predicted $\log K_I$ in Tables 1 and 2) can still be obtained by fitting the experimental data for mono- and divalent negative oxygen donor ligands. Indeed, as follows from Fig. 2, the theoretically calculated $\log K_I$ values show a very strong correlation with the experimental data (coefficients of determination: (a) $R^2 = 0.953$ and (b) $R^2 = 0.938$). Linear regression analysis suggests the following derived regression equations (a) and (b):

$$\log K_I^{\text{expt}} = 0.272 \times \log K_I^{\text{calc}} \quad (\text{a})$$

$$\log K_I^{\text{expt}} = 0.390 \times \log K_I^{\text{calc}} - 1.583, \quad (\text{b})$$

which essentially correct for deficiencies introduced by the solvation model and possess a significant predictive power. For the predicted $\log K_I$ values, the root-mean-square errors (RMSE) are only 0.53 (VO^{2+}) and 0.85 (VO_2^+) log units, respectively, confirming that the

presented computational method can provide accurate and reliable estimates of the absolute stability constant values for 1:1 complexes with vanadium species.

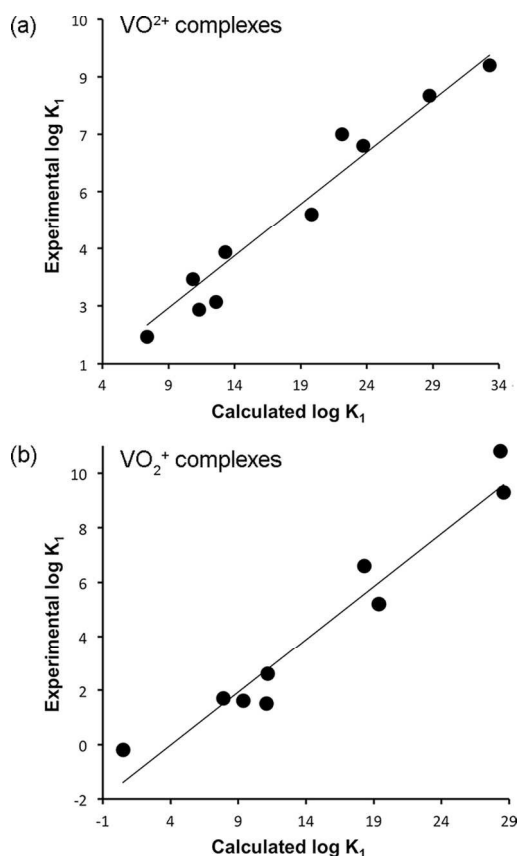


Fig. 2. Plots of experimental vs. calculated $\log K_1$ values in aqueous solution for corresponding (a) oxovanadium (IV) and (b) dioxovanadium (V) complexes with oxygen donor ligands. Equations for the regression lines: (a) $\log K_1^{\text{expt}} = 0.272 \times \log K_1^{\text{calc}}$, with $R^2 = 0.953$; (b) $\log K_1^{\text{expt}} = 0.390 \times \log K_1^{\text{calc}} - 1.583$, with $R^2 = 0.938$.

The difference between $\log K_1$ values for uranyl and oxovanadium ions can be used to assess the degree of ligand selectivity toward UO_2^{2+} vs. $\text{VO}^{2+}/\text{VO}_2^+$. However, it is worth noting that the predicted $\log K_1$ values can deviate from experimental $\log K_1$ values, with absolute errors of more than 1.0 log unit in some cases (Tables 1, 2, and ref. 33,42). Since our main goal is to predict accurately the selectivity for UO_2^{2+} over $\text{VO}^{2+}/\text{VO}_2^+$ ions, it is important to check whether our predictions follow the experimental selectivity trend. Thus, we compared the predicted and experimental $\log K_1$ values for UO_2^{2+} , VO^{2+} , and VO_2^+ complexes with the same ligands. Histograms in Fig. 3 verify that our theoretical results are generally in agreement with

the experimental data, suggesting that the developed computational protocols for oxovanadium ions in conjunction with the analogous approach for predicting the stability constants for uranyl complexes^{33,42} can be a useful means of screening for new ligands with strong chelating capability to UO_2^{2+} .

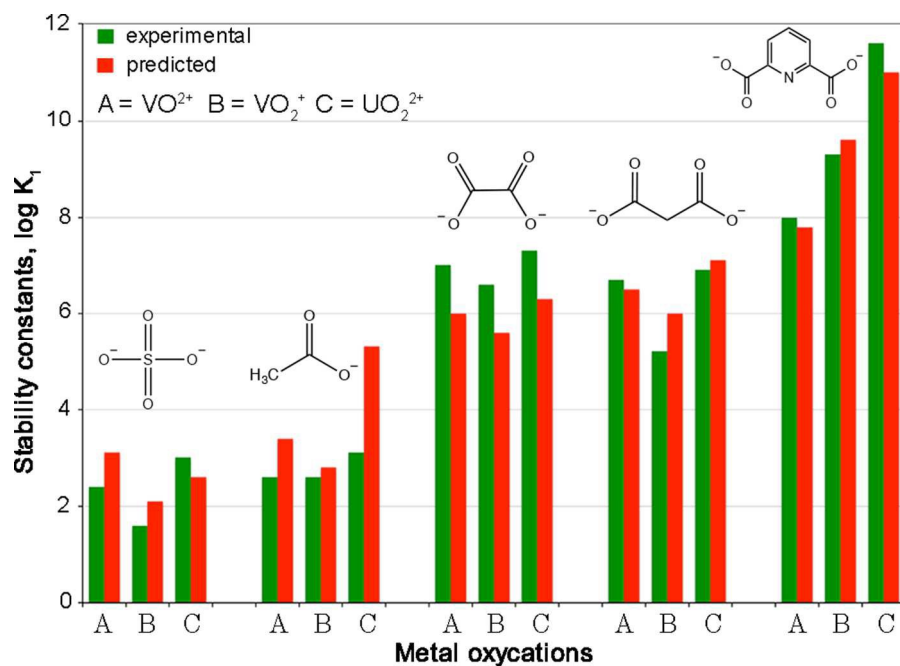
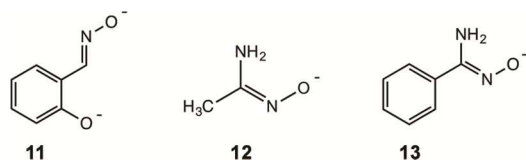


Fig. 3. Histograms showing comparison of experimental (green) and predicted (red) $\log K_1$ values for A) VO^{2+} , B) VO_2^+ , and C) UO_2^{2+} complexes with identical ligands.

Table 3. Predicted $\log K_1$ Values for Oxovanadium (IV), Dioxovanadium (V), and Uranyl Complexes with Oxime Ligands.



ligand	pred. ^a $\log K_1$ VO^{2+}	pred. ^a $\log K_1$ VO_2^+	pred. ^b $\log K_1$ UO_2^{2+}	expt. ^c $\log K_1$ UO_2^{2+}
11 salicylaldoximate	5.8	4.2	17.2	16.1
12 acetamidoximate	9.2	10.4	13.4	13.6
13 benzamidoximate	8.5	9.4	12.2	12.4

^aPredicted from equations derived from regressions shown in Fig. 2.

^bRef. 42.

^cRef. 42,45. The corresponding experimental data for the VO^{2+} and VO_2^+ complexes are not available.

Having developed a $\log K_f$ calculation method that achieves good accuracy, we can now begin to examine the trends in selectivity for potential ligands that would possess higher binding affinity to UO_2^{2+} vs. VO^{2+} and VO_2^+ ions. Amidoxime based ligands are of special interest because of their ability to extract uranium under seawater conditions.^{11-13,18,20,22} Oxime ligands – amidoxime analogs but with a proton in place of the amine – are also of potential interest because they can preserve the oximate group, which is capable of η^2 coordinating with uranyl,^{18,43} and at the same time eliminate the stabilizing effect of amine coordination observed in the representative crystal structures of amidoxime complexes with transition metal ions.⁴⁴ Additionally, it was recently demonstrated that salicylaldoximate (Sal) ligand (structure **11** in Table 3) showed one of the greatest binding affinities to UO_2^{2+} (Table 3) while retaining a high selectivity for uranium over Fe^{3+} and Cu^{2+} cations.⁴² However, the selectivity of salicylaldoxime for UO_2^{2+} versus VO^{2+} and VO_2^+ ions has not been assessed, since experimental $\log K_f$ values for the corresponding complexes have not been reported. The results of the $\log K_f$ calculations for salicylaldoxime ligand are summarized in Table 3.

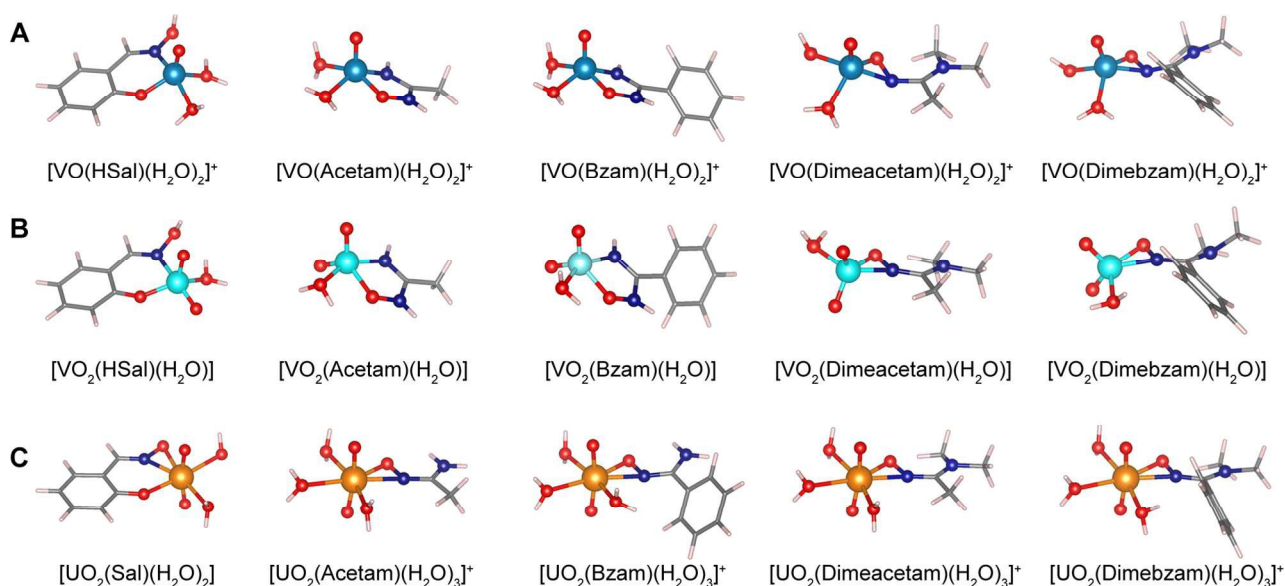


Fig. 4. Optimized geometries for aqueous 1:1 metal oxycation-ligand complexes. Color legend: O, red; N, navy blue; C, grey; H, white; V(IV), blue; V(V), turquoise; U, orange.

Consistent with previous work on salicylaldoxime binding to the Cu^{2+} cation,⁴² salicylaldoxime- $\text{VO}^{2+}/\text{VO}_2^+$ complexes are formed *via* coordination of the phenolate group and the nitrogen atom of the oxime group (Fig. 4, structures $[\text{VO}(\text{HSal})(\text{H}_2\text{O})_2]^+$ and $[\text{VO}_2(\text{HSal})(\text{H}_2\text{O})]$, respectively). However, salicylaldoxime coordinates with UO_2^{2+} as a dianion species formed by η^2 coordination of the aldoximate and monodentate binding of the phenolate group (Fig. 4, structure $[\text{UO}_2(\text{Sal})(\text{H}_2\text{O})_2]$).⁴² Thus, the predicted higher UO_2^{2+} vs. $\text{VO}^{2+}/\text{VO}_2^+$ selectivity of salicylaldoxime can likely be attributed to the inability of smaller vanadium ions to accommodate simultaneous binding of the oximate and the phenolate functional groups. As one may see from Table 3, UO_2^{2+} complexes ($\log K_I = 17.2$) are ~ 11 – 13 orders of magnitude stronger than corresponding VO^{2+} ($\log K_I = 5.8$) and VO_2^+ ($\log K_I = 4.2$) complexes with salicylaldoxime, indicating that this ligand is a very promising candidate for selective extraction of uranium from seawater.

While the synthesis and subsequent grafting of new ligands on a polymer fiber is a time consuming process, optimizing the current poly(acrylamidoxime) sorbent characteristics to favor uranium vs. vanadium sorption is a more straightforward task. Thus, we decided to examine the binding affinity to VO^{2+} and VO_2^+ for typical amidoxime ligands: acetamidoxime (Acetam) and benzamidoxime (Bzam) (Table 3, structures **12** and **13**, respectively), both of which can be present in poly(acrylamidoxime) sorbents depending on the synthesis conditions. Although experimental and theoretical studies have been performed to establish stability constants and to describe the interaction between these ligands and uranyl,⁴⁵ a comparison of the predicted stability constants for UO_2^{2+} and $\text{VO}^{2+}/\text{VO}_2^+$ has not been made. The results of the calculations for Acetam and Bzam ligands are shown in Table 3. As one may see, the $\log K_I$ values for VO^{2+} and VO_2^+ are ~ 3 – 4 log units lower than those for UO_2^{2+} , meaning that amidoximes should be more selective toward uranyl. However, recent experimental studies demonstrate much higher vanadium adsorption capacity of amidoxime-based fibers in natural seawater.⁴⁶ Such a discrepancy between experimental and theoretical results can be explained by the fact that in the actual adsorbent polymer, amidoxime groups adjacent to each other tend to form cyclic imide dioximes (Scheme S1 of the ESI[†]), which may be the actual sorption sites for uranyl and other competing ions, including vanadium.⁴⁷ The seminal work by Rao et al.⁴⁸ provides additional arguments suggesting that the high sorption of VO_2^+ by the poly(amidoxime) sorbents is probably due to the strong interaction between VO_2^+ and cyclic imide dioxime. These

interactions lead to the formation of the very stable and rare V^{5+} non-oxido complex.⁴⁸ It has also been suggested that in order to improve the selectivity of the sorbent for UO_2^{2+} over VO_2^+ , a perfect ligand should have sufficiently high binding affinity for uranyl and low binding affinity for vanadium, so it would not be possible to displace the oxido bonds in VO_2^+ . As follows from the results in Table 3, acyclic amidoxime ligands (**12** and **13**) conform to these requirements. However, the substitution of both amine hydrogen atoms with alkyl groups is needed to prevent possible cyclization processes of the amidoxime ligands in the actual adsorbent polymer. Previous computational and experimental studies demonstrated that amidoxime complexes with UO_2^{2+} and VO^{2+}/VO_2^+ represent different binding motifs. Although η^2 (side-on) coordination of the oxime functional group is preferred by UO_2^{2+} ,¹⁸ the most stable binding motif for VO^{2+}/VO_2^+ entails the chelate coordination of oxime oxygen and amide nitrogen atoms via a tautomeric rearrangement of amidoxime to imino hydroxylamine (Fig. 4).^{39,40} Thus, alkylamidoxime-binding groups such as N,N-dimethylamidoximes, which cannot undergo tautomerization, are expected to display even greater selectivity for uranium by eliminating the favorable vanadium-binding (chelate) pathway. To test this concept, we applied our computational method to the alkyl-substituted Acetam and Bzam ligands (Fig. 4). The calculated selectivity of UO_2^{2+} over VO^{2+}/VO_2^+ (Fig. 5), given by the ratio of the equilibrium constants for the corresponding UO_2^{2+} and VO^{2+}/VO_2^+ complexation reactions, indicates that N,N-dimethylamidoximes would possess even higher separation ability (without compromising strong binding affinity to UO_2^{2+}) than their unsubstituted counterparts. Therefore, the proposed alkylation of amidoximes could be a potential route to better discrimination between uranyl and vanadium ions within seawater. Experimental testing of this new design strategy is currently underway in our laboratory.

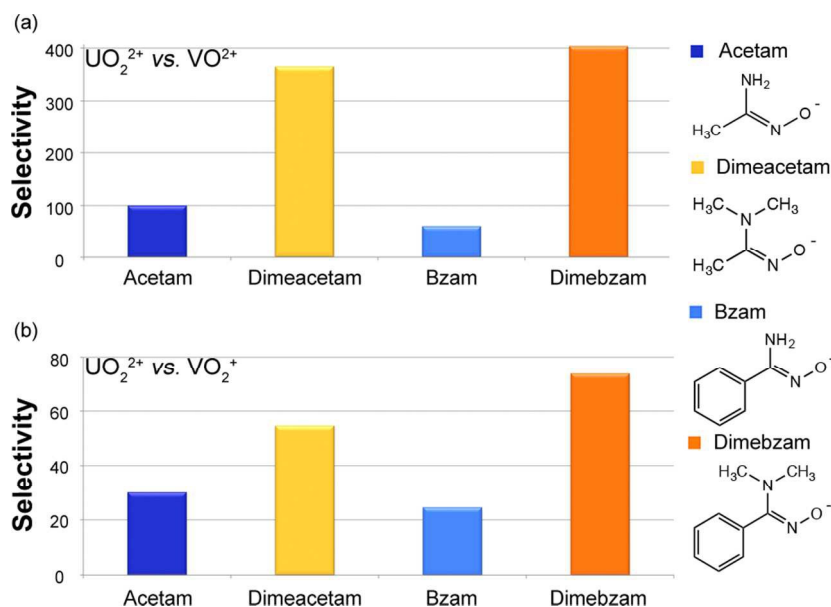


Fig. 5. Ligand selectivity for UO_2^{2+} over (a) VO_2^{2+} and (b) VO_2^+ ions. Ligands: acetamidoximate (Acetam); N,N-dimethylacetamidoximate (Dimeacetam); benzamidoximate (Bzam) and N,N-dimethylbenzamidoximate (Dimebzm).

CONCLUSION

The molecular design of novel chelating agents within a polymer fiber that possess high binding affinity and selectivity toward uranyl *vs.* vanadium species plays an important role in increasing sorption capacity of existing adsorbents. A key step in predicting ligand selectivity and efficiency at sequestering uranium is the ability to accurately predict the $\log K_f$ values for the uranyl and major competing VO_2^{2+} and VO_2^+ ions. In this work, we have presented computational protocols, developed for VO_2^{2+} and VO_2^+ complexes, that yield good accuracy (root-mean-square error < 0.85 log units) by employing linear least-squares fitting of the calculated $\log K_f$ values to the experimental data for ten negative oxygen donor ligands. In conjunction with the recently developed analogous approach for predicting the stability constants of uranyl complexes,³³ this work provides the essential foundation for prospective screening of existing or even yet unsynthesized ligands with higher selectivity for uranium over vanadium. This is particularly significant when considering whether to make an otherwise highly attractive ligand that may be synthetically challenging. If such a ligand is predicted by our calculations to achieve the desired uranium *versus* vanadium selectivity, this substantially reduces the risk of taking on such

synthetic challenges. Moreover, the elimination of ligands that are unlikely to show a good uranyl binding affinity can release resources to focus on more promising UO_2^{2+} -selective ligands. We note, however, that molecular modeling results presented in this work describe uranium and vanadium complexation in ideal solution under zero ionic strength. Thus, when the theoretically proposed ligand is grafted on a fiber, its ability of selectively sequestering uranyl could be somewhat altered under real seawater conditions.

The stability constants for uranium complexes with salicylaldoxime were calculated to be noticeably higher than those of vanadium, thereby suggesting that salicylaldoxime is a promising candidate for the selective extraction of uranium from seawater. In addition, the developed computational protocols could be used to confirm the proposed design principles for improving the current generation of amidoxime-derived sorbents. As follows from our results, substituting both amine hydrogen atoms of amidoxime ligands can indeed increase the selectivity for uranium by eliminating the favorable vanadium-binding pathway and preventing the formation of cyclic imide dioxime, which is likely responsible for the higher sorption of vanadium ions in marine tests. Overall, extensive deployment of the presented computational approaches in UO_2^{2+} -selective ligand discovery is expected to lead to more rapid completion of difficult projects related to the extraction of uranium from seawater, with potentially superior adsorbent materials as an end result.

ASSOCIATED CONTENT

†Electronic supplementary information (ESI) available: sample Gaussian 09 input file, performance of CCSD(T)/aug-cc-pvDZ//B3LYP/aug-cc-pvDZ calculations for $\text{VO}^{2+}/\text{VO}_2^+$ complexes with acetate and oxalate ligands, scheme of conversion of poly(acrylamidoximes) to poly(acrylimidedioximes) under basic conditions, and Cartesian coordinates of ligands and metal-ligand complexes obtained with B3LYP functional. See DOI: 10.1039/x0xx00000x

FUNDING

This research was sponsored by the U.S. Department of Energy, Office of Nuclear Energy under Contract DE-AC05-00OR22725 with Oak Ridge National Laboratory, managed by UT-Battelle,

LLC. This manuscript has been authored by UT- Battelle, LLC under Contract DE-AC05-00OR22725 with the U.S. Department of Energy.

ACKNOWLEDGMENTS

The authors thank Dr. Jerry M. Parks (ORNL) for critically reading the manuscript and offering helpful suggestions. This research used resources of the National Energy Research Scientific Computing Center, a DOE Office of Science User Facility supported by the Office of Science of the U.S. Department of Energy under Contract No. DE-AC02-05CH11231.

REFERENCES

- 1 U.S. Nuclear Regulatory Commission. *Final Generic Environmental Impact Statement on Uranium Milling*; U.S. Nuclear Regulatory Commission; Washington, DC, 1980; NUREG-0706.
- 2 OCED, Uranium 2014: Resources, Production, and Demand, 2014.
- 3 R. V. Davies, J. Kennedy, R. W. McIlroy, R. Spence and K. M. Hill, *Nature*, 1964, **203**, 1110.
- 4 D. L. Clark, D. E. Hobart and M. P. Neu, *Chem. Rev.*, 1995, **95**, 25.
- 5 J. D. Wilson, R. K. Webster, G. W. C. Milner, G. A. Barrett and A. A. Smales, *Anal. Chim. Acta*, 1960, **23**, 505.
- 6 I. Tabushi, Y. Kobuke and T. Nishiya, *Nature*, 1979, **280**, 665.
- 7 A. C. Q. Ladeira and C. A. Morais, *Minerals Eng.*, 2005, **18**, 1337.
- 8 P. S. Kulkarni, S. Mukhopadhyay, M. P. Bellary and S. K. Ghosh, *Hydrometallurgy*, 2002, **64**, 49.
- 9 R. S. S. Murthy and D. E. Ryan, *Anal. Chem.*, 1983, **55**, 682.
- 10 T. Takeda, K. Saito, K. Uezu, S. Furusaki, T. Sugo and J. Okamoto, *Ind. Eng. Chem. Res.*, 1991, **30**, 185.
- 11 M. Tamada, N. Seko, N. Kasai and T. Shimizu, *Trans. At. Energy Soc. Japan*, 2006, **5**, 358.

- 12 I. Tabushi, Y. Kobuke and T. Nishiya, *Nature*, 1979, **280**, 665.
- 13 M. J. Kanno, *Nucl. Sci. Technol.*, 1984, **21**, 1.
- 14 J. Kim, C. Tsouris, Y. Oyola, C. J. Janke, R. T. Mayes, S. Dai, G. Gill, L.-J. Kuo, J. Wood, K.-Y. Choe, E. Schneider and H. Lindner, *Ind. Eng. Chem. Res.*, 2014, **53**, 6076.
- 15 *Fuel Cycle Technologies Annual Review Meeting Transactions Report, INL/EXT-14-33501, FCRD-FCT-2015-000003*, Idaho National Laboratory, Idaho Falls, Idaho 83415, 2015.
<http://www.inl.gov>
- 16 J. Kim, C. Tsouris, R. T. Mayes, Y. Oyola, T. Saito, C. J. Janke, S. Dai, E. Schneider and D. Sachde, *Sep. Sci. Technol.*, 2013, **48**, 367.
- 17 T. Suzuki, K. Saito, T. Sugo, H. Ogura and K. Oguma, *Anal. Sci.*, 2000, **16**, 429.
- 18 S. Vukovic, L. Watson, S. O. Kang, R. Custelcean and B. P. Hay, *Inorg. Chem.*, 2012, **51**, 3855.
- 19 G. Tian, S. J. Teat, Z. Zhang and L. Rao, *Dalton Trans.*, 2012, **41**, 11579.
- 20 S. Vukovic and B. P. Hay, *Inorg. Chem.*, 2013, **52**, 7805.
- 21 C. F. Xu, J. Su, X. Xu and J. Li, *Sci. China: Chem.*, 2013, **56**, 1525.
- 22 C. Z. Wang, J.-H. Lan, Q. Y. Wu, Q. Luo, Y. L. Zhao, X. K. Wang, Z. F. Chai and W. Q. Shi, *Inorg. Chem.*, 2014, **53**, 9466.
- 23 C. Priest, Z. Q. Tian and D. E. Jiang, *Dalton Trans.*, DOI:10.1039/c5dt04576b.
- 24 C. W. Abney, S. Liu and W. Lin, *J. Phys. Chem. A*, 2013, **117**, 11558.
- 25 M. J. Frisch, G. W. Trucks, H. B. Schlegel, G. E. Scuseria, M. A. Robb, J. R. Cheeseman, G. Scalmani, V. Barone, B. Mennucci, G. A. Petersson, H. Nakatsuji, M. Caricato, X. Li, H. P. Hratchian, A. F. Izmaylov, J. Bloino, G. Zheng, J. L. Sonnenberg, M. Hada, M. Ehara, K. Toyota, R. Fukuda, J. Hasegawa, M. Ishida, T. Nakajima, Y. Honda, O. Kitao, H. Nakai, T. Vreven, J. A. Montgomery, Jr., J. E. Peralta, F. Ogliaro, M. Bearpark, J. J. Heyd, E. Brothers, K.

N. Kudin, V. N. Staroverov, R. Kobayashi, J. Normand, K. Raghavachari, A. Rendell, J. C. Burant, S. S. Iyengar, J. Tomasi, M. Cossi, N. Rega, M. J. Millam, M. Klene, J. E. Knox, J. B. Cross, V. Bakken, C. Adamo, J. Jaramillo, R. Gomperts, R. E. Stratmann, O. Yazyev, A. J. Austin, R. Cammi, C. Pomelli, J. W. Ochterski, R. L. Martin, K. Morokuma, V. G. Zakrzewski, G. A. Voth, P. Salvador, J. J. Dannenberg, S. Dapprich, A. D. Daniels, Ö. Farkas, J. B. Foresman, J. V. Ortiz, J. Cioslowski and D. J. Fox, *Gaussian 09 Revision D.01*, Wallingford, CT, Gaussian, Inc., 2009.

26 A. D. Becke, *J. Chem. Phys.*, 1993, **98**, 5648.

27 C. Lee, W. Yang and R. G. Parr, *Phys. Rev. B*, 1988, **37**, 785.

28 Y. Zhao and D. G. Truhlar, *Theor. Chem. Acc.*, 2008, **120**, 215.

29 M. Dolg, H. Stoll, H. Preuss and R. M. Pitzer, *J. Phys. Chem.*, 1993, **97**, 5852.

30 R. F. Ribeiro, A. V. Marenich, C. J. Cramer and D. G. Truhlar, *J. Phys. Chem. B*, 2011, **115**, 14556.

31 A. V. Marenich, C. J. Cramer and D. G. Truhlar, *J. Phys. Chem. B*, 2009, **113**, 6378.

32 S. Chatterjee, S. Brown, J. C. Johnson, C. D. Granta, R. T. Mayes, B. P. Hay, V. S. Bryantsev, S. Dai and T. Saito, *Ind. Eng. Res. Chem.*, 2015, (DOI: 10.1021/acs.iecr.1025b03212).

33 S. Vukovic, B. P. Hay and V. S. Bryantsev, *Inorg. Chem.*, 2015, **54**, 3995.

34 X. Sun, C. Xu, G. Tian and L. Rao, *Dalton Trans.*, 2013, **42**, 14621.

35 S. P. Kelley, P. S. Barber, P. H. Mullins and R. D. Rogers, *Chem. Comm.*, 2014, **50**, 12504.

36 C. J. Leggett, F. Endrizzi and L. Rao, *Ind. Eng. Chem. Res.*, **2016**, DOI: 10.1021/acs.iecr.5b03688.

37 (a) NIST Standard Reference Database 46. NIST Critically Selected Stability Constants of Metal Complexes Database, version 8.0; Data collected and selected by Smith, R. M., Martell, A.

E.; US Department of Commerce, National Institute of Standards and Technology: Gaithersburg, MD, 2004. (b) The IUPAC Stability Constants Database; Academic Software: Yorks, UK, <http://www.acadsoft.co.uk/scdbase/scdbase.htm>.

38 C. W. Davies, *Ion Association*; Butterworths: Washington, DC, 1962.

39 N. Mehio, J. C. Johnson, S. Dai and V. S. Bryantsev, *Phys. Chem. Chem. Phys.*, 2015, **17**, 31715.

40 N. Mehio, A. S. Ivanov, A. P. Ladshaw, S. Dai and V. S. Bryantsev, *Ind. Eng. Res. Chem.*, 2015, DOI: 10.1021/acs.iecr.5b03398.

41 V. S. Bryantsev, M. S. Diallo and W. A. Goddard III, *J. Phys. Chem. A*, 2009, **113**, 9559.

42 N. Mehio, A. S. Ivanov, N. J. Williams, R. T. Mayes, V. S. Bryantsev, R. D. Hancock and S. Dai, *Dalton. Trans.*, 2016, DOI: 10.1039/C6DT00116E.

43 P. S. Barber, S. P. Kelley, P. H. Mullins and R. D. Rogers, *RSC Adv.*, 2012, **2**, 8526.

44 (a) G. A. Pearse Jr and R. T. Pflaum, *J. Am. Chem. Soc.*, 1959, **81**, 6505; (b) D. L. Cullen and E. C. Lingafelter, *Inorg. Chem.*, 1970, **9**, 1865; (c) H. Endres, *Acta Cryst.*, 1982, **B38**, 1313; (d) C. D. Stout, M. Sundaralingam and G. H. Y. Lin, *Acta Cryst.*, 1972, **B28**, 2136.

45 M. A. Lashley, N. Mehio, J. W. Nugent, E. Holguin, C.-L. Do-Thanh, V. S Bryantsev, S. Dai and R. D. Hancock, *Polyhedron*, 2016, DOI:10.1016/j.poly.2016.01.026.

46 S. Das, W.-P. Liao, M. Flicker Byers, C. Tsouris, C. J. Janke, R. T. Mayes, E. A. Schneider, L.-J. Kuo, J. Wood and G. A. Gill, et al. *Ind. Eng. Chem. Res.* 2015, DOI: 10.1021/acs.iecr.5b03210.

47 (a) A. Zhang, T. Asakura and G. Uchiyama, *React. Funct. Polym.*, 2003, **57**, 67; (b) S. O. Kang, S. Vukovic, R. Custelcean and B. P. Hay, *Ind. Eng. Res. Chem.*, 2012, **51**, 6619.

48 C. J. Leggett, B. F. Parker, S. J. Teat, Z. Zhang, P. D. Dau, W. W. Lukens, S. M. Peterson, A. J. P. Cardenas, M. G. Warner, J. K. Gibson, J. Arnold and L. Rao, 2016, DOI: 10.1039/C5SC03958D.

Table of Contents

Synopsis: Computational assessment of $\log K_l$ values leads to novel design strategies for improving the ligand selectivity towards UO_2^{2+} vs. $\text{VO}_2^{2+}/\text{VO}_2^+$.

